

Thermal falling film modelling validation and exploration

N. Cellier^a, Philippe Bandelier^b, Nadia Caney^c, Benoit Stutz^a,
C. Ruyer-Quil^{a,d}

a. CNRS - Université Savoie Mont-Blanc - LOCIE

b. Commissariat à l'énergie atomique et aux énergies alternatives - LETI

c. CNRS - Université Grenoble Alpes - LEGI

d. Institut Universitaire de France

Résumé :

Les transferts de chaleur à travers un film ruisselant sur une plaque chauffée dépendent non seulement des caractéristiques thermiques du fluide mais aussi des caractéristiques de l'écoulement : les travaux expérimentaux de la littérature montrent que la présence d'instabilités hydrodynamiques peuvent mener à des intensifications de transfert non négligeable par rapport au cas d'un film d'épaisseur uniforme.

Un modèle asymptotique à 4 équations fondé sur une méthode aux résidus pondérés a été formulé précédemment dans le cas des transferts de chaleur [11]. Il s'agira de valider ce modèle en le comparant à une résolution directe de l'équation de Fourier par une méthode pseudo-spectrale, puis d'identifier les phénomènes responsables de cette intensification.

Abstract :

Heat transfer across the film on a heated plate are not only functions of thermal characteristics of the film but also of the flow conditions. Experimental works show an enhancement of heat transfer when the hydrodynamical instabilities occur compared to a flat film.

A 4 equations asymptotic model based on a weighted residual method has been developed previously [11]. This work aims at validating this model by comparisons with the Fourier equation solved by a pseudo-spectral method, and at deciphering the mechanisms leading to the heat intensification.

Keywords : transfer intensification, heat exchangers, falling films, free surface instabilities

1 Introduction

1.1 Context & motivation

The development of appropriate solar energy storage at building scale with sorption technologies requires compact and versatile heat exchangers operating with low temperature sources. Traditional designs used in industrial contexts (e.g. tubular exchangers) are not suitable for the aimed application.

Falling-film plate exchangers constitute an appropriate alternative : wavy films lead to exchange intensification which results from enhanced liquid thinning and efficient mixing due to wave merging [12, 3]. Frisk and al. [4], and more recently Gonda and al. [5], have shown a similar heat transfer intensification across an unstable falling film. Previous works based on the long-wave expansion show that these phenomena can be captured by a shallow water like model developed with a weighted residual method [6]. A three-equation model (with the film thickness h , the local flow-rate q and the surface temperature θ as dependent variables of the problem) has shown some non-physical behavior at high Biot number and above a given Peclet number : the temperature of the film goes outside its physical bounds. An earlier attempt show that this failure can not be corrected with only three variables [2]. To that aim, a new four equations model has been proposed by introducing a new variable related to the wall flux [11]. This work is an attempt to provide extra validation of this model and to explore the interaction between hydrodynamics and heat transfer within a heated falling film.

1.2 Physical system

The system studied is a thin layer of fluid flowing down an inclined bottom as sketched in figure 1. Full wettability is assumed. The temperature at the hot plate is constant and corresponds to a unit dimensionless value. The temperature at the atmosphere is equal to zero, so that the temperature field lies in the range : $T \in [0, 1]$.

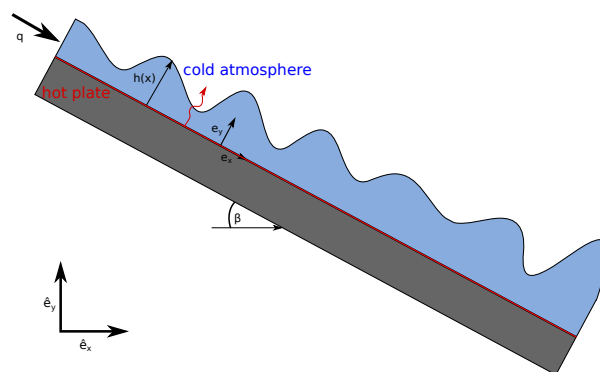


FIGURE 1 – Falling films on heated plate

1.3 Dimensionless numbers and scaling of the system

The relevant thermo-physical properties are the following :

ν the kinematic viscosity ($\text{m}^2 \text{s}^{-1}$)

ρ the liquid density (kg m^{-3})

P_∞ the atmosphere pressure (Pa)

β the inclination between the wall and the horizontal plane (rad)

λ the liquid film diffusion coefficient ($\text{W m}^{-1} \text{K}^{-1}$)

α the heat transfer coefficient between the film and the atmosphere ($\text{W m}^{-2} \text{K}^{-1}$)

T_∞ the atmosphere temperature (K)

T_w the wall temperature (K)

g the gravitational acceleration (m s^{-2})

The simplest solution of our system, referred to hereinafter as Nusselt solution, is a film of uniform thickness $h = \bar{h}_N$. This solution is always unstable whenever the wall is vertical ($\beta \neq \frac{\pi}{2}$) or the Reynolds number exceeds a critical value $Re_c = \frac{5}{6}Ct$.

Based on the length scale \bar{h}_N the flow conditions are represented by the following dimensionless numbers :

Re the Reynolds number, based on the averaged velocity $Re = \frac{\bar{u}_N \bar{h}_N}{\nu} = \frac{g \sin \beta \bar{h}_N}{3\nu^2}$

We the Weber number $We = \frac{\sigma_\infty}{\rho g \bar{h}_N^2 \sin \beta} = \frac{\Gamma}{(3Re)^{2/3}}$ where $\Gamma = \frac{\sigma_\infty}{\rho(g \sin \beta)^{1/3} \nu^{4/3}}$ is the Kapitza number.

Ct the inclination number $Ct = \cot \beta$

Pe the Peclet number $Pe = PrRe$ where $Pr = \frac{\nu}{\chi}$ is the Prandtl number.

Bi the Biot number $Bi = \frac{\alpha \nu^{2/3}}{\lambda(g \sin \beta)^{1/3}}$

2 Modelling

2.1 4 equations thermal model

For consistency we recall the 4 equations model formulated previously [11].

$$\partial_t h = -\partial_x q \quad (1a)$$

$$3Re \partial_t q = \frac{5}{6} h (1 - Ct \partial_x h + We \partial_{xxx} h) - \frac{5}{2} \frac{q}{h^2} + 3Re \left(\frac{9}{7} \frac{q^2}{h} \partial_x h - \frac{17}{7} \frac{q}{h} \partial_x q \right) \quad (1b)$$

$$3Pe \left(\partial_t + \frac{3q}{2h} \partial_x \right) \theta = \frac{180}{17h^2} - \frac{12[-15 + (15 + 8Bi)h]}{17h^2} \theta + \frac{7}{17h^2} \varphi + \frac{9}{2} \partial_{xx} q - \frac{9}{2} \frac{\partial_x h \partial_x q}{h} + 4 \frac{\partial_x h^2 q}{h^2} - 6 \frac{\partial_{xx} h q}{h} \quad (1c)$$

$$3Pe h \partial_t (\varphi/h) = -\frac{460}{17h^2} - \frac{120[-4 + (4 + Bi)h]}{17h^2} \theta + \frac{3}{17h^2} \varphi + \partial_{xx} \varphi + \left[-\frac{\varphi}{17} \right] \frac{\partial_{xx} h}{h} + \left[J_{\varphi, \theta} - \frac{56\varphi}{17} + J_\varphi \right] \frac{(\partial_x h)^2}{h^2} - \frac{120}{17} \frac{\partial_x h \partial_x \theta}{h} - \frac{22}{17} \frac{\partial_x h \partial_x \varphi}{h} \quad (1d)$$

The system (1) is formed of 4 evolution equations for the following dependent variables : the film elevation h , the local flow rate q , the temperature at the free surface θ and the wall flux $\frac{\phi}{h} = \partial_y T|_{y=0}$. The coefficients J_i are functions of Bi and h only.

The derivation of (1) is based on the long-wave nature of the instabilities of the film. As a wavy regime develops along the film, the typical length of the waves, L , is much larger than the typical thickness \bar{h}_N

of the film. This large aspect ratio enables to introduce a small parameter $\varepsilon = \frac{\bar{h}_N}{L}$. Basic equations have thus been truncated at $\mathcal{O}(\varepsilon)$ by dropping higher order terms and then averaged across the film thickness with appropriate weights in order to retain consistency up to order $\mathcal{O}(\varepsilon)$ at least, i.e. at $\mathcal{O}(\varepsilon)$ for inertial or convective terms and $\mathcal{O}(\varepsilon^2)$ for diffusion terms.

Equation (1a) is the exact local mass balance, (1b) is a truncated averaged momentum equation. Equations (1c) and (1d) are deduced from the weighted heat balance averaged across the film and represent the evolution of the temperature field.

Numerical integration of system (1) has been performed using centered finite differences.

2.2 Full Fourier model

The velocity field is computed from the usual self-similar assumption, where the stream-wise velocity is supposed to remain locally close to the Nusselt solution with a parabolic profile (2) [10].

$$u = 3\frac{q}{h} \left[\frac{y}{h} - \frac{1}{2} \left(\frac{y}{h} \right)^2 \right] \quad v = - \int \partial_x u dy \quad (2)$$

We numerically solve the Fourier equation :

$$3\text{Pe} (\partial_t T + u\partial_x T + v\partial_y T) = \partial_{xx} T + \partial_{yy} T \quad (3)$$

With a fixed temperature at the wall and a Newton cooling law at the free surface :

$$T|_{y=0} = 1 \quad (4a)$$

$$\partial_y T|_{y=h} = -\text{Bi}T|_{y=h} \quad (4b)$$

The discretization across the film uses a ten Tchebychev polynomial interpolation on the Gauss-Lobatto nodes. The boundary conditions are taken into account by basis recombination [1]. This leads to a ten equation system (h , q , and 8 bulk temperatures evaluated at the Gauss-Lobatto nodes, the free surface and wall temperature being obtained from the boundary conditions). Discretization in the stream-wise direction is next achieved using centered finite differences.

Numerical consideration Solutions are found using the method of line, the spacial derivatives being first discretize and the resulting ODE system being solved using standard methods for large dynamical systems. The spatial discretization is obtained with a computer algebra system (CAS) and optimizing compiler tools (sympy¹ and theano² libraries) in order to achieve a fast computation of the time derivative vector and its Jacobian matrix. The integration in time is performed via an implicit 6th order Rosenbrock-Wanner scheme as described in [9] with an adaptive time stepping to fulfill both stability and accuracy conditions.

1. <http://www.sympy.org/en/index.html/>

2. <http://deeplearning.net/software/theano/>

3 Results

3.1 Validation

An extensive numerical study have been undertaken by varying two parameters, the Biot and the Prandtl numbers, the other ones being held constant and equal to $Ct = 0$, $Re = 15$, $We = 268.8$. This choice corresponds to specific flow conditions, namely a water film on a vertical plate. The distribution of the Biot and Prandtl number is represented in figure 2 and has been generated using a Latin Hypercube Sampling (LHS) method [8].

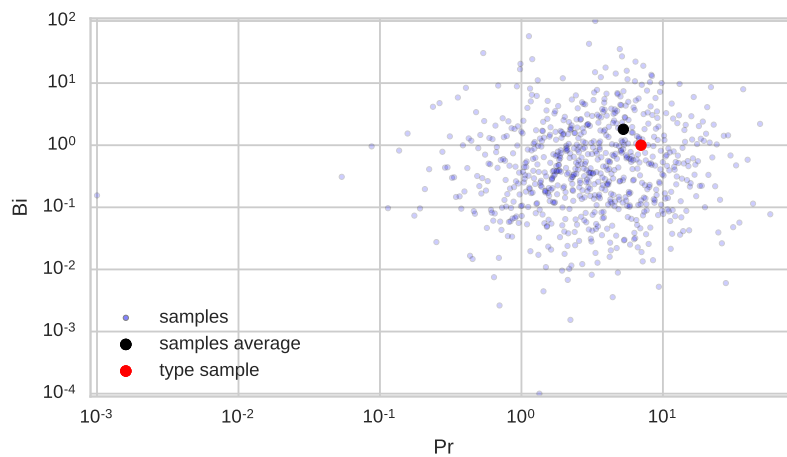


FIGURE 2 – Sample distribution in the free parameter space Biot vs. Prandtl numbers

Figures 3 and 4 sum up the relative and absolute error for the θ and ϕ values of each sample.

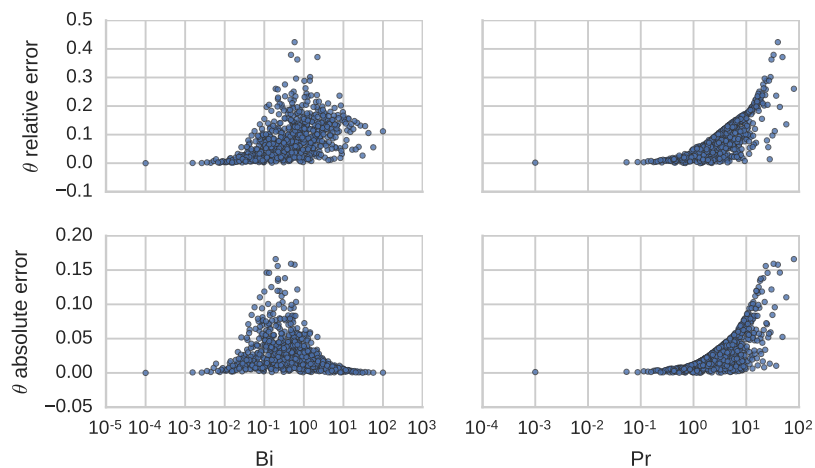


FIGURE 3 – θ relative and absolute errors distribution according to the Bi and Pr number.

The maximum of the error is strongly correlated to the Prandtl number. This result is expected as the long-wave expansion assumed that convective terms are dominated by the cross-stream diffusion ones, which hold only if the Peclet number ($Pe = Re Pr$) remains of $O(1)$.

Besides the error distributions show marked peaks at Biot number in the range 0.1 to 1. This corresponds closely to the onset of thermal boundary layers in the hump regions of the waves, which drastically

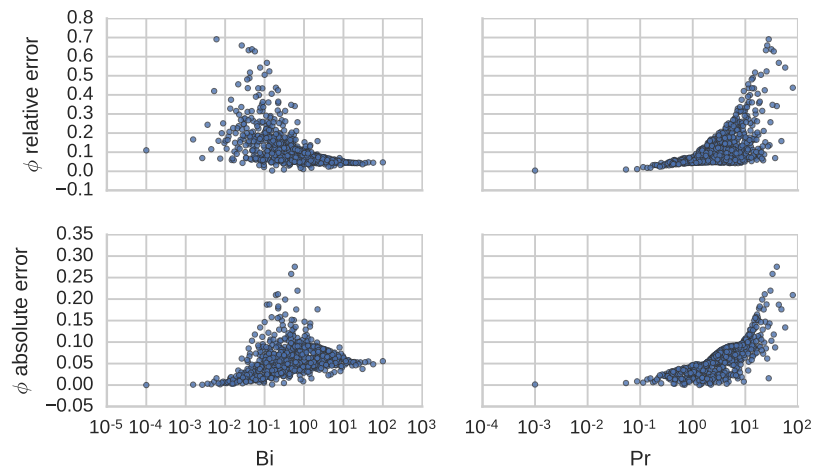


FIGURE 4 – ϕ relative and absolute errors distribution according to the Bi and Pr number.

complicates the temperature profile across the film. For this reason our model of reduced dimensionality experiences difficulty to quantitatively reproduce the temperature field in this case. Yet for most relevant situations ($Pr \leq 7$) the relative errors remain below the acceptable limit of 15%.

3.2 Exploration

We present preliminary results on the effect of the hydrodynamic regime on the heat transfer. To this aim, simulations in an extended domain representative of a plate element are performed. The inlet boundary condition mimics the application of a periodic forcing on the inlet flow-rate and includes a certain amount of natural noise. The outlet boundary conditions limits the reflexion of the incoming waves and includes an absorbent buffer zone in order to approach as closely as possible to the open-flow situation.

The parameters of the simulation correspond to the water film situation validated previously ($Ct = 0$, $Re = 15$, $We = 268.8$).

By varying the forcing frequency, we observe the following regimes (some of them are represented in figure 5) :

- With very low frequency, the film is not locked to the input frequency, natural waves take over.
- Increasing the frequency and the film amplify the input frequency, and a train wave will appear with enough space to be fully developed.
- At some point, the waves are too close to exhibit capillary waves : train of single hump wave are then observed up to the point where the waves become purely sinusoidal with a low amplitude which correspond to the critical linear frequency of the film.
- As still higher frequencies, inlet forcing becomes ineffective and natural waves dominate again.

Simulations have been conducted for a low value of Biot number ($Bi = 0.1$) representative of a heat exchanger with cold atmosphere. The frequencies are evenly sampled between 0.5 and 40 Hz. The liquid is introduced at ambient temperature. The Reynolds number is chosen to be moderate ($Re = 15$) but the Prandtl number is taken relatively large. This choice enables to reproduce accurately the hydrodynamics of the flow as demonstrated in [7] at a value of the Peclet number which is representative of the operating conditions of a plate exchanger.

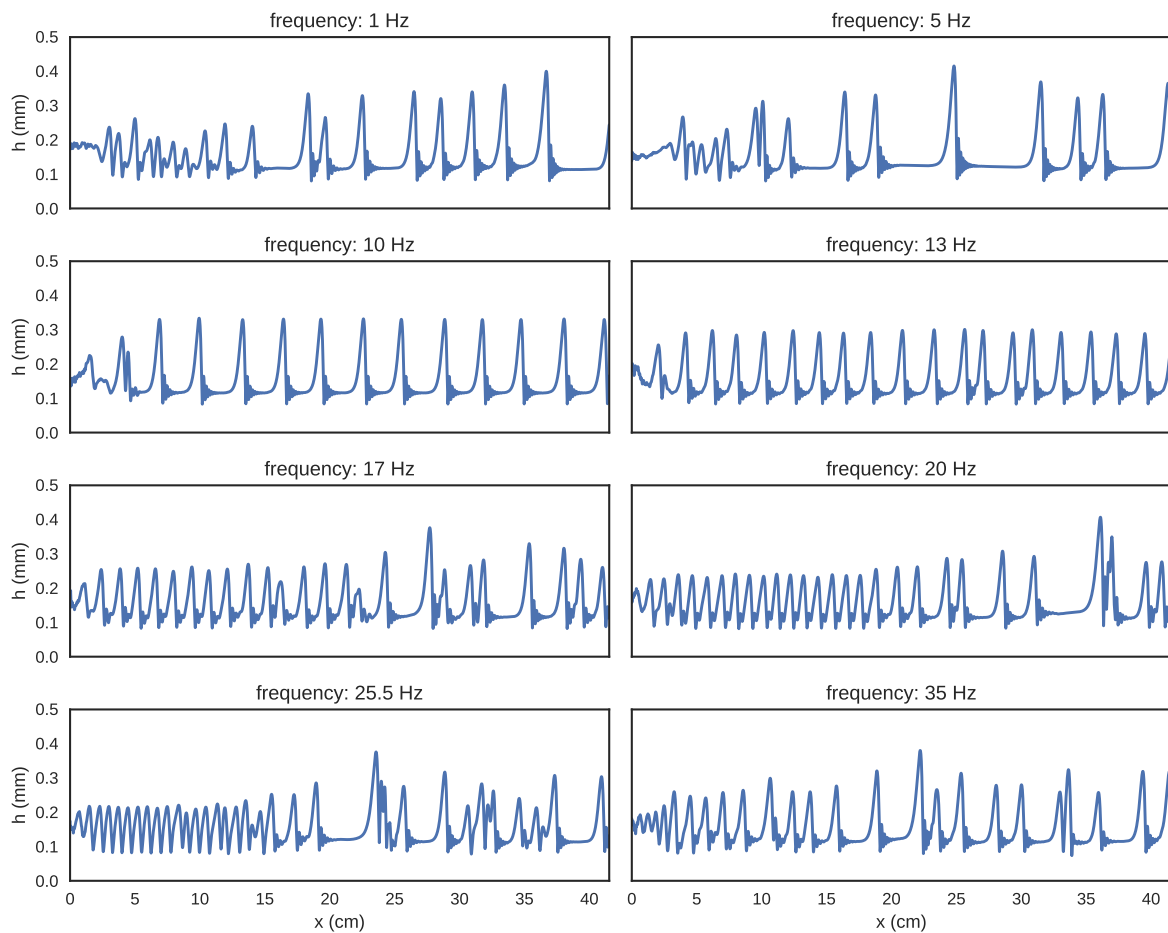


FIGURE 5 – snapshot of the film thickness along the plate for different inlet forcing frequencies
 $Ct = 0$, $Re = 15$, $We = 268.8$

The heat transfer enhancement has been measured by computing the global Nusselt number based on the total flux exchanged at the wall along the whole numerical domain and averaged in time :

$$Nu = \frac{\langle \int_0^L \phi(x) dx \rangle}{\phi_{\text{flat film}} \cdot L}$$

Time averaging has been conducted after simulations were performed for a certain time so that the initial transient evolution of the flow is evacuated. Figure 6 displays the evolution of the Nusselt number as a function of the inlet forcing frequency. For all tested frequencies a significant enhancement of heat transfer by the waves is observed. At low frequencies results seem rather scattered which is a signature of the fact that the averaging was performed on a too limited time window with respect to the characteristic evolution time of the system. For such low frequencies we anticipate this time to be rather long. For instance, for the frequency $f = 0.5$ Hz the averaging was chosen to last 10 seconds, the period of the forcing is 2 seconds and the crossing time of the Nusselt flow is 3.3 seconds. At higher frequencies, results are far less scattered. A peak is observed at $f \approx 13$ Hz where a strong synchronization of the flow with inlet frequency is achieved, with very regular wave-trains. At still higher frequencies the Nusselt number decreases to a plateau as wave-trains become more and more disordered with the onset of secondary instabilities. The response of the film is then analogous to the

natural evolution of the film generated by a white noise at inlet.

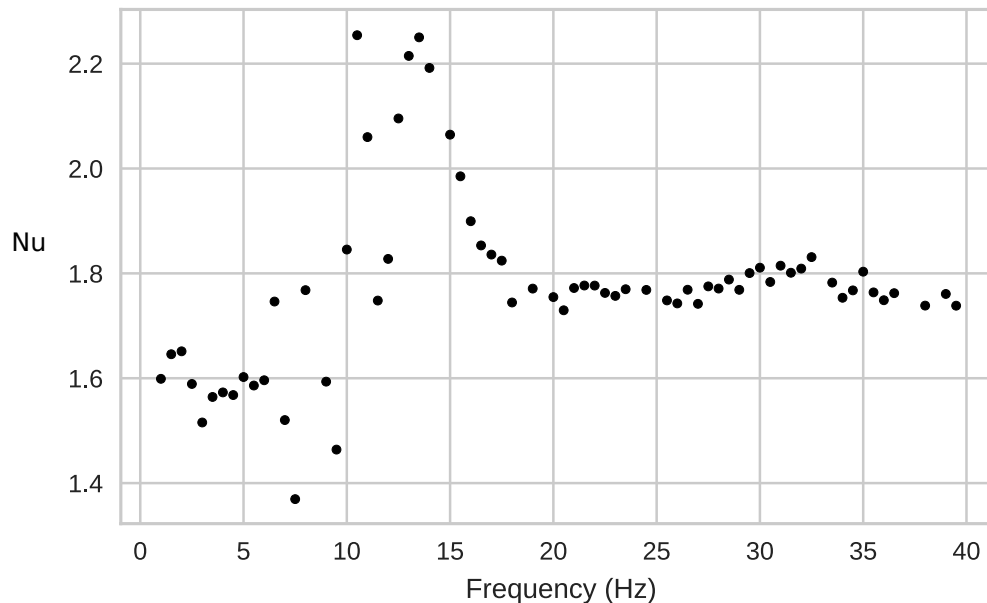


FIGURE 6 – Heat enhancement across the film according to the input frequency
 $Ct = 0$, $Re = 15$, $We = 268.8$, $Pr = 35$, $Bi = 0.1$

4 Conclusion

Simulations of heat transfer across a falling film on a vertical plate have been performed in an extended numerical domain which is representative of an element of a falling-film plate heat exchanger. Parameters and boundary conditions have been chosen according to experiment conditions.

The 4-equation model derived in [11] has been validated through comparisons with the solutions to the Fourier equation showing an acceptable level of inaccuracies for typical values of the parameters.

Extensive numerical simulations have shown a significant enhancement of the heat transfer resulting from the onset of the wavy regime. A noticeable dependency of the Nusselt number with respect to the forcing frequency has been observed. Interestingly, the natural dynamics of the film is not the most favorable case for the heat transfer. In contrast, the maximum of the Nusselt number is reported to occur when synchronization to the inlet frequency is achieved all along the plate, which corresponds to a quite narrow range of frequencies.

Références

- [1] J. P. Boyd. Chebyshev and Fourier Spectral Methods. *New York*, page 688, 2000.
- [2] M. Chhay, D. Dutykh, M. Gislou, and C. Ruyer-Quil. Asymptotic heat transfer model in thin liquid films. *Submitted*, pages 1–24, 2015.
- [3] G. F. Dietze and C. Ruyer-Quil. Wavy liquid films in interaction with a confined laminar gas flow. *J. Fluid Mech*, 722 :348–393, 2013.

- [4] D. P. Frisk and E. J. Davis. The enhancement of heat transfer by waves in stratified gas-liquid flow. *International Journal of Heat and Mass Transfer*, 15(8) :1537–1552, aug 1972.
- [5] A. Gonda, P. Lancereau, P. Bandelier, L. Luo, Y. Fan, and S. Benezech. Water falling film evaporation on a corrugated plate. *International Journal of Thermal Sciences*, 81(1) :29–37, 2014.
- [6] S. Kalliadasis, C. Ruyer-Quil, B. Scheid, and M. G. Velarde. *Falling Liquid Films*, volume 176 of *Applied Mathematical Sciences*. Springer London, London, 2012.
- [7] N. Kofman, C. Ruyer-Quil, and S. Mergui. Selection of solitary waves in vertically falling liquid films. *International Journal of Multiphase Flow*, 84 :75–85, 2016.
- [8] M. D. McKay, R. J. Beckman, and W. J. Conover. A Comparison of Three Methods for Selecting Values of Input Variables in the Analysis of Output from a Computer Code. *Technometrics*, 21(2) :239, may 1979.
- [9] J. Rang. Improved traditional Rosenbrock–Wanner methods for stiff ODEs and DAEs. *Journal of Computational and Applied Mathematics*, 286 :128–144, 2015.
- [10] C. Ruyer-Quil and P. Manneville. Improved modeling of flows down inclined planes. *The European Physical Journal B*, 15(2) :357–369, 2000.
- [11] C. Ruyer-Quil, B. Stutz, M. Chhay, and N. Cellier. Instabilités hydrodynamique et thermocapillaire d’un film liquide tombant à grand nombre de Péclet - 22ème congrès français de Mécanique [CFM2015] - Lyon, 24 au 28 Août 2015.
- [12] P. N. Yoshimura, T. Nosoko, and T. Nagata. Enhancement of mass transfer into a falling laminar liquid film by two-dimensional surface waves—Some experimental observations and modeling. *Chemical Engineering Science*, 51(8) :1231–1240, apr 1996.